

Article

Observation and Manipulation of a Capillary Jet in a Centrifuge-Based Droplet Shooting Device

Kazuki Maeda ^{1,†}, Hiroaki Onoe ^{1,2,‡}, Masahiro Takinoue ³ and Shoji Takeuchi ^{1,2,*}

Received: 1 September 2015 ; Accepted: 3 October 2015 ; Published: 10 October 2015

Academic Editor: Marc Madou

¹ Institute of Industrial Science, the University of Tokyo, 4-6-1 Komaba, Meguro-ku, Tokyo 153-8505, Japan; maeda@caltech.edu (K.M.); onoe@mech.keio.ac.jp (H.O.)

² Takeuchi Biohybrid Innovation Project, Exploratory Research for Advanced Technology (ERATO), Japan Science and Technology (JST), Komaba Open Laboratory (KOL) Room M202, 4-6-1 Komaba, Meguro-ku, Tokyo 153-8904, Japan

³ Department of Computational Intelligence and Systems Science, Tokyo Institute of Technology, 4259-G3-53 Nagatsuta-cho, Midori-ku, Yokohama, Kanagawa 226-8502, Japan; takinoue@dis.titech.ac.jp

* Correspondence: takeuchi@iis.u-tokyo.ac.jp; Tel.: +81-3-5452-6650; Fax: +81-3-5452-6649

† Present address: Department of Mechanical Engineering, California Institute of Technology, 1200 E California Blvd, Pasadena, CA 91125, USA.

‡ Present address: Department of Mechanical Engineering, Faculty of Science and Technology, Keio University, 3-14-1 Hiyoshi, Kouhoku-ku, Yokohama, Kanagawa 223-8522, Japan.

Abstract: We report observation and manipulation of a capillary jet under ultra-high centrifugal gravity in a proposed capillary-based fluidic device for the synthesis of microparticles in a centrifugal tube called *Centrifuge-Based Droplet Shooting Device* (CDSD). Using a high-speed camera, we directly observed the dripping to jetting transition of a viscous capillary jet of water and Sodium alginate solution generated from a glass capillary-orifice of a diameter of $O(100)$ μm under centrifugal gravity ranging from 190 to 450 g . A non-dimensional analysis shows that the mechanism of the dripping-jetting transition in the CDSD may follow that previously reported for a dripping faucet under standard gravity. We also fabricated calcium alginate microparticles by gelating droplets of sodium alginate solution obtained in the break-up of the capillary jet in the jetting regime and demonstrated fabrication of microbeads-on-a-string structures. We confirmed that the jetting regime of the capillary jet could be used to fabricate smaller particles than that of the dripping regime. The results show that the CDSD would be a more useful device to fabricate various polymeric structures and understand the physics of fluid jets under ultra-high gravity.

Keywords: microfluidics; centrifuge; high-speed visualization; polymeric particles

1. Introduction

Manipulation and gelation of polymer liquid flow in microfluidic devices is a powerful approach to produce micro-particles for various applications such as multiplexing assay [1,2], platforms for biological analysis [3], photonic devices [4], drug carriers [5], and scaffolds for tissue engineering [6]. Microfluidic devices, such as T-junction [7] and flow-focusing [8] often use a system of co-flowing immiscible liquid for stable production of monodisperse polymeric droplets/particles. In those systems, a flow of immiscible liquid such as silicon oil is introduced into that of polymer liquid in a micro channel to co-flow in a way that the polymer flow is focused and broken into micro-sized droplets by hydrodynamic instability. To equip the micro channels in a precise configuration in the devices, special setups for micro device fabrication are often required. Additionally, to control flow rates of the polymer and immiscible liquid streams in the devices, external pumps need to be attached.

Recently, we have reported a centrifuge-based droplet shooting device (CDSD), a capillary-based fluidic device for the synthesis of microparticles in a centrifugal tube [9]. In the CDSD, the flow of a sodium alginate solution is ejected from a glass capillary nozzle by centrifugal gravity and forms droplets. The droplets gelate directly in a CaCl_2 solution located at the bottom of the tube. The size of the capillary nozzle, the gravity, and the solution are directly tunable. All the processes of particle fabrication are conducted in a centrifugal tube rotating in a centrifuge. This simple technique enables particle fabrication without the need for a special environment, additional immiscible liquid or an external pump. In our previous work, we reported the high capability of the CDSD to fabricate multi-compartmental particles simply by using a multi-barreled capillary. However, the process of droplet formation itself has not yet been fully addressed, despite the fact that it is an engineering basis of the device and the key to enhance the feasibility of the device's applications.

In this paper, we report on the systematic analyses of the droplet formation from a capillary jet under non-standard ultra-high gravity in the CDSD using high-speed videography and fabrication of calcium alginate microparticles. We confirmed that the drop formation from a capillary jet in the CDSD can transition between dripping regime and jetting regime by changing the centrifugal gravity. Through a non-dimensional analysis, we confirmed that the mechanism of the dripping-jetting transition in the CDSD may follow that reported by Ambravaneswaran *et al.* [10] for a dripping faucet under standard gravity. Moreover, we confirmed that flows in the jetting regime supply smaller particles than in the dripping regime. Taking advantage of these analyses, we also controlled the size of the particles obtained in the jetting regime by varying the diameter of the capillary orifice. Lastly, we demonstrated fabrication of beads-on-a-string structures by gelating the capillary jet of the sodium alginate solution. The observational analysis of the dripping-jetting transition, and the fabrication of microparticles and microstructures in the CDSD, suggests its versatility for fabrication of polymeric particles and structures of various sizes. Additionally, there is potential for use as a device to understand the physics of droplet formation from a liquid flow under non-standard ultra-high gravity.

2. Experimental Section

2.1. Materials

In all of the particle fabrication experiments, the particle material was sodium alginate solution. A 500 mM CaCl_2 solution was used to gelify the solution. The sodium alginate was purchased from Wako Pure Chemicals Industries, Ltd. (Osaka, Japan). The CaCl_2 was purchased from Kanto Chemicals Co., Ltd. (Tokyo, Japan).

2.2. Analysis of the Dripping-Jetting Transition

Figure 1 shows a set up for the observation of liquid jet formation in the CDSD. The setup was composed of a nano-pulse stroboscope, a magnetic pickup sensor, a trigger circuit, a centrifuge equipped with the CDSD, and a microscope connected to a high-speed camera. When a centrifuge rotor passed near the sensor, a voltage was created in the sensor by electromagnetic induction. The trigger circuit converted the voltage to a stable square wave that activated the stroboscope, causing it to emit a strobe flash from a strobe guide under the CDSD. The CDSD was set to pass under the focal point of the microscope at the same moment. Thus, when the strobe flash was pulsed, the capillary jet in the CDSD under the strobe flash was captured with the camera through the microscope. The duration of the strobe flash was 180 ns. This short flash duration enabled videography of resolutions finer than 2 μm in a 2000 rpm centrifugation. A liquid tank was connected to the capillary in the CDSD to deduce the flow rate of the capillary jet by measuring the change of the liquid volume. A detailed description of the setup is shown in Figure S1.

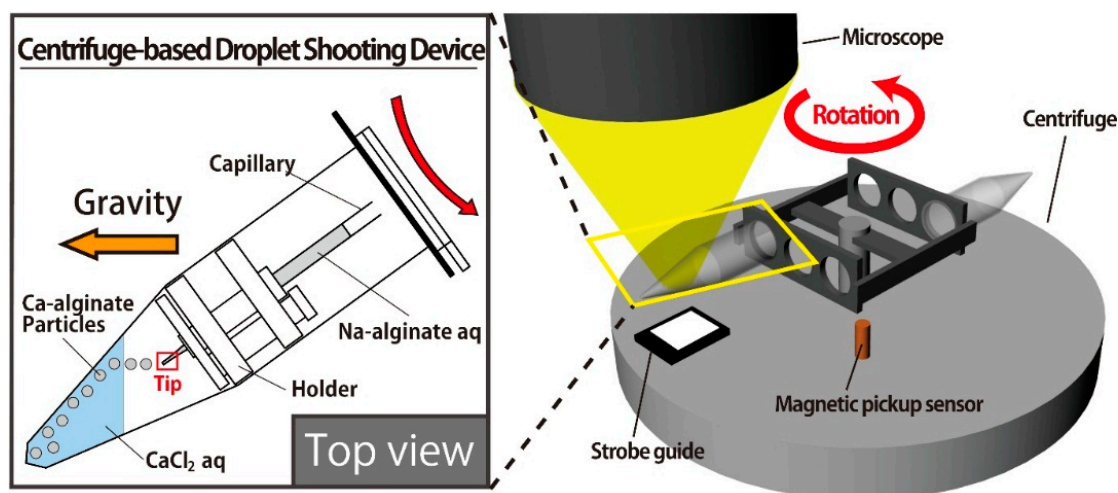


Figure 1. Schematic depiction of the setup for observation of the capillary jet.

2.3. Particle Fabrication in the Jetting Regime

Particles were fabricated by gelation of droplets consisting of 2.0% (*w/w*) sodium alginate solutions ejected from a capillary ($d_p = 113, 120, 130$ and $140\ \mu\text{m}$) in the CaCl_2 solution.

2.4. Beads-On-A-String Structure Fabrication

The beads-on-a-string structure was fabricated by gelation of a capillary jet consisting of a 1.5% (*w/w*) sodium alginate solution in the CaCl_2 solution using a capillary with $d_c = 120\ \mu\text{m}$. The distance between the capillary orifice and the surface of the CaCl_2 solution was set to 4 mm.

3. Results and Discussion

3.1. Analysis of the Dripping-Jetting Transition

The transition between dripping and jetting regimes, or dripping–jetting transition, is now a widely confirmed fascinating physical phenomenon in the droplet formation of Newtonian fluids [10–12]. At a slow flow rate, the release of liquid in the dripping regime is sustained at the nozzle by surface tension in the form of a pendant drop. When the force of gravity surpasses the surface tension, the pendant drop detaches from the nozzle, and a droplet is formed [13]. As the flow rate increases, the droplet formation process undergoes a transition to the jetting regime at a certain threshold. In the jetting regime, a liquid flow ejected from the nozzle forms a liquid pipe, which becomes a sequence of droplets far from the nozzle owing to the Rayleigh–Plateau instability [14]. The dripping–jetting transition is also important for applications of droplet production since the size of the droplets varies in the dripping and jetting regimes [15]. Using the observational setup, we captured both the jetting and dripping regimes of droplet formation. In the dripping regime (Figure 2a), droplets were formed at the capillary orifice and detached by centrifugal gravity when the volume of the droplet increased and the gravitational force acting on the drop surpassed the counteracting surface tension force exerted from the capillary orifice. When we increased the centrifugal gravity and the liquid flow rate exceeded a certain threshold, the flow switched to the jetting regime (Figure 2b) in which the liquid ejected from the capillary in the form of a fluid pipe eventually broke up into droplets. Likewise, the flow in the jetting regime switched back to the dripping regime at a certain point as the flow rate was lowered.

Through videography, we analyzed the dripping–jetting transition using water and sodium alginate solutions of various concentrations with capillaries of various diameters by changing the flow rate. Following a 1-D model introduced by Ambravaneswaran *et al.* (2002) [16], we expressed the dynamics of the capillary jet with three dimensionless parameters: the Bond number (Bo), the Ohnesorge number (Oh), and the Weber number, (We). In our system, $Bo \equiv \rho d_c^2 g / \sigma$, $Oh \equiv \mu / \sqrt{\rho d_c \sigma}$, and $We \equiv \rho U^2 d_c / \sigma$, where ρ is the liquid density; σ is the surface tension; d_c is the diameter of the inner capillary orifice; μ is the liquid viscosity; g is the centrifugal gravity; and U is the liquid flow rate. Figure 3 depicts a phase diagram, based on We and Oh showing the critical pairs of We and Oh experimentally obtained where the dripping–jetting transitions occurred when we gradually raised the flow rate from the dripping regime by increasing the centrifugal rotation speed. The range of g and Bo at the transition was $190\text{ g} < g < 450\text{ g}$ and $0.15 < Bo < 1.0$. The values of the dimensionless numbers at each point of the transition are shown in Table S1 and Table S2. Figure 3 shows that when $Oh \sim 1$, the transition occurred at $We \sim 0.1$, whereas the critical We at which the transition occurred monotonically increased to ~ 0.8 as Oh decreased by a factor of 100. Though We is a function of Bo as well as of Oh , the range of Bo is smaller compared to that of Oh in order of magnitude. For this reason, following Ambravaneswaran *et al.* [10], we assume that the effect of Bo on the dripping–jetting transition is modest. Based on the studies of dependency of relevant time scale for capillary breakup on Ohnesorge number [17], Ambravaneswaran *et al.* [10] argued that when $Oh \ll 1$, the transition occurs at $We \sim O(1)$, while the We at the transition decreases as Oh increases, in accordance with their experimental and simulation results in which the jetting-to-dripping transition occurs at $We \sim O(1)$ when $Oh \ll 1$ and the critical We at which the transition occurs monotonically decreases as Oh increases. The profile of the separation in the dimensionless space between the jetting and dripping phases in Figure 3 is in accordance with the above argument. Thus, the present study may suggest that the mechanism of dripping–jetting transition in a viscous flow released in an ambient gas driven by a range of centrifugal gravity satisfying $Bo \sim 1$ could follow that of the transition driven by standard gravity in a stationary environment. In our system, without centrifugal gravity, owing to the small capillary size, $Bo \sim 10^{-4}$, and the dripping–jetting transition could not occur in the same fashion as for $Bo \sim 1$. To realize the dripping–jetting transition using a small capillary in a simple way, introduction of centrifugal gravity could be a valuable approach. In the present experiments, the direction of the flows is altered at the capillary orifice due to the configuration of the centrifuge, as shown in Figure 2a,b. However, this alternation of the flow direction would have a minimal effect on the present analysis of the dripping–jetting transition based on the 1-D model.

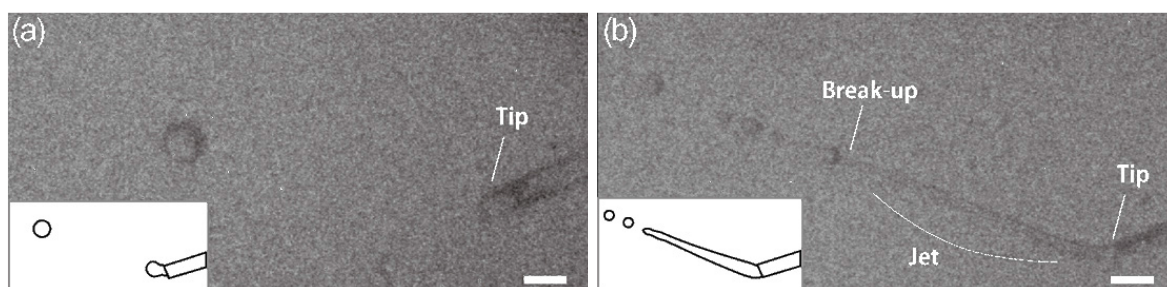


Figure 2. Observed capillary jet in a Centrifuge-Based Droplet Shooting Device (CDSD): (a) Dripping regime; (b) Jetting regime. The insets depict schematic images of the dripping (a), and jetting (b), observed. The scale bars are 200 μm .

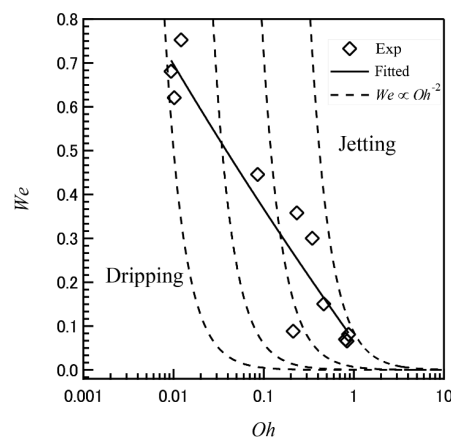


Figure 3. Experimentally obtained phase diagram in (We, Oh) space.

3.2. Particle Fabrication in the Jetting Regime

Figure 4a shows the obtained particles when $d_c = 120 \mu\text{m}$. Figure 4b shows $d_p \propto d_c$. This linear correlation between d_p and d_c in the jetting regime corresponds to that explained by the Plateau–Rayleigh instability of a capillary fluid pipe ejected into the air that spontaneously breaks up into droplets [18]. At the capillary orifice, we may assume $U \propto \mu^{-1}$ due to the following reasons: the flow in the capillary can be regarded as being steady and unidirectional; the flow is laminar since $Re < O(10^2)$ at the capillary orifice in all the experimental conditions, where Re is the Reynolds number defined as $Re \equiv \rho d_c U / \mu = \sqrt{We} / Re$; we assume that the flow is fully developed since the ratio of total capillary and tube length to the capillary cross-sectional diameter is sufficiently large (>50) [19]. In our system, if $U \propto \mu^{-1}$, $We \propto Oh^{-2}$ when ρ , d_c , and σ are fixed. In Figure 3, the dotted lines that represent $We \propto Oh^{-2}$ monotonically decrease and intersect the approximated border between the two phases. Thus, in the range of Bo addressed in the present study, if surface tension and density are the same, a liquid jet of fluid with higher viscosity would tend to approach the dripping regime, compared to that of less viscous fluid released from a capillary orifice of the same diameter. As we previously reported in the dripping regime, we have the correlation $d_p \propto d_c^{1/3}$ [9]. Therefore, introduction of a capillary with a thin orifice and a high centrifugal gravity that produces the jetting regime could miniaturize particles more than that of the dripping regime. The particles obtained by the jetting regime in the present study is relatively polydispersed (coefficient of variation (CV): 15.0% for those in Figure 4a), compared to those obtained by the dripping regime in the CDSD (CV: 2.0% [1]). This polydispersity could be due to the unsteady fluid dynamic process of the droplet formation in the jetting regime, in contrast to the that of the dripping regime; the instability of the capillary jet that causes droplet formation in the jetting regime should be largely fluctuated by external disturbances, such as the subtle mechanical vibration of the centrifuge, whereas in the dripping regime droplet size can be determined by a quasi-steady balance between the surface tension and the gravitational force acting on the pendant drop at the capillary orifice [9]. Since other devices utilizing hydrodynamic instability to produce particles, including T-junction and flow-focusing, produce monodispersed particles [8,20], we could enhance the uniformity of the particle size obtained the jetting regime in the CDSD by improving the precision of the device setup to suppress the disturbances. It should be noted that the transition from the jetting to dripping regimes occurring when we decrease the flow rate of the capillary jet at the jetting regime by lowering centrifugal gravity, is not addressed in the present study. Due to hysteresis, the jetting–dripping transition would occur at lower We than that of dripping–jetting transition if plotted on the Oh – We phase diagram shown in Figure 3 [10]. Furthermore, as reported by Rubio-Rubio *et al.* [12] on the jetting–dripping transition of capillary from a vertically oriented tube in the range of $We < 0.1$, the effect of Bo would not be negligible on the jetting–dripping transition at low We .

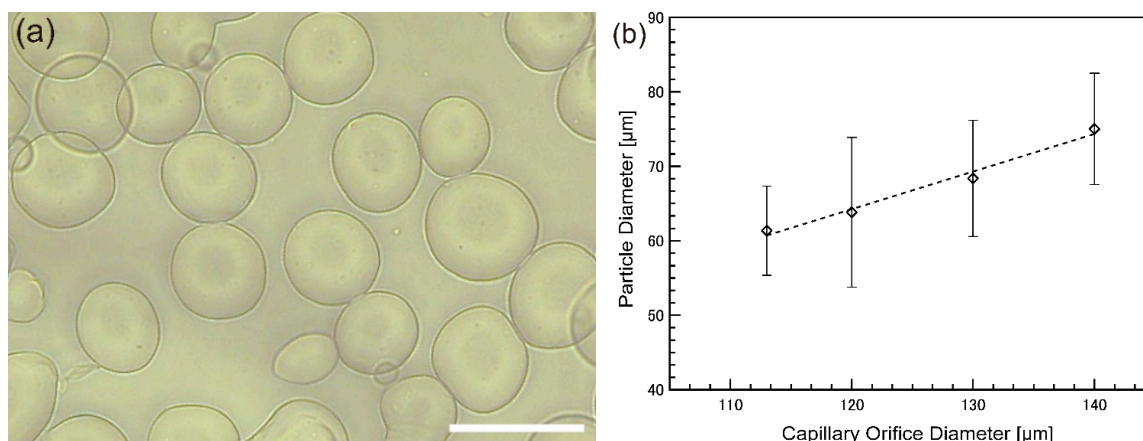


Figure 4. Fabricated particles and size control in a jetting regime: (a) A microscopic image of particles obtained through gelation of 2.0% (*w/w*) sodium alginate droplets ejected from a capillary with an orifice of $d_c = 120 \mu\text{m}$ in the CaCl_2 solution. The scale bar is $100 \mu\text{m}$. The mean particle diameter is $68 \pm 10 \mu\text{m}$, and $n = 100$; (b) The correlation between d_p and d_c when droplets of 2.0% (*w/w*) sodium alginate solutions gelate in the CaCl_2 solution.

3.3. Beads-on-a-String Structure Fabrication

By gelation of the capillary jet of sodium alginate solution in the jetting regime at the position where the jet break-up took place, we fabricated microbeads-on-a-string structures. The process of the gelation was not directly observed due to the difficulty directly capturing the image of the surface of CaCl_2 solution. However, as shown in Figure 5a, we surmised that during the break-up caused by hydrodynamic instability, the capillary jet formed a thin neck between the drop and the jet pipe. The structure of drops connected by necks entered the CaCl_2 solution before complete break-up, and the structure gelled with its shape maintained, owing to the instantaneous gelation. Figure 5b shows the resultant microbeads-on-a-string structures. The strings connecting the microbeads reached nanometer-scale, as shown in the inset of Figure 5b. It is well known that a thin thread of viscous liquid forms the microbeads-on-a-string structure as seen in glue or a spider web [21]. Capillary-jet break-up and related physics owing to hydrodynamic instability have been of great interest for decades [14,15,22–25]. Our techniques of instantaneous gelation of the capillary-jet structure during break-up could enable the observation of an unstable fluid structure in a stable fashion under ambient conditions without any special instruments or observational setup other than a microscope.

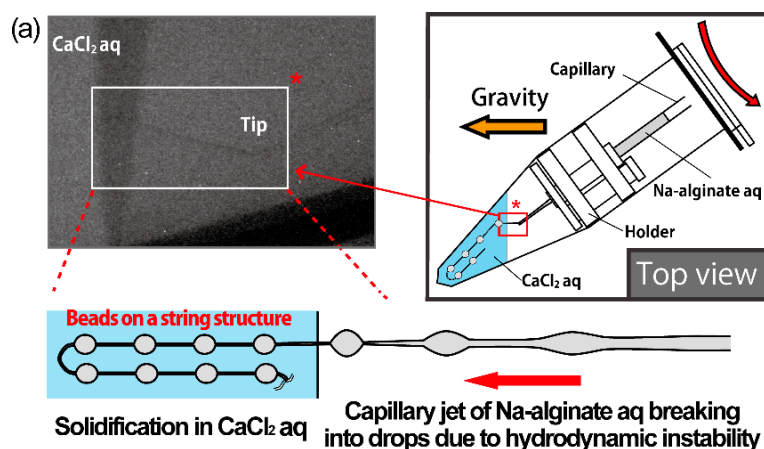


Figure 5. Cont.

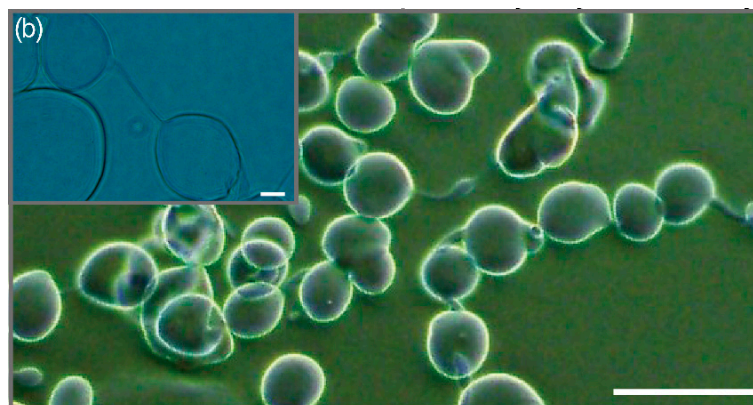


Figure 5. Beads-on-a-string structure made of calcium alginate: (a) Schematic diagram of the formation process of the beads-on-a-string structure. Viscous capillary jet of Na-alginate solution under deformation due to hydrodynamic instability directly gelled in the CaCl_2 solution before complete break-up; (b) Fabricated beads-on-a-string structures. The inset shows the string connecting the microbeads as small as sub-micron scale in thickness. The scale bars are 10 μm in the inset and 100 μm in the main frame.

4. Conclusions

We analyzed the dripping-jetting transition of a capillary jet under non-standard ultra-high gravity in the CDS, fabricated calcium alginate microparticles by gelation of droplets of sodium alginate solution obtained in the break-up of the capillary jet in the jetting regime, controlled the particle size by varying the capillary orifice diameter, and demonstrated fabrication of microbeads-on-a-string structures. Through the non-dimensional analysis based on observation of the capillary jet in the CDS using a nano-pulse stroboscope, we confirmed that the dripping-jetting transition under centrifugal acceleration may follow the physics previously reported for a dripping faucet under standard gravity. To the best of our knowledge, this is the first observational analysis of a viscous capillary jet driven by centrifugal acceleration. Moreover, we confirmed that, unlike the dripping regime, the jetting regime in which the particle diameter was proportional to the diameter of the capillary orifice, may enable further miniaturization of particles by introducing a capillary with a thinner diameter and a higher centrifugal gravity. The present study suggests the potential of the CDS being used to fabricate various types of polymeric particles and structures as well as to understand physics of the capillary jet under non-standard ultra-high gravity.

Supplementary Materials: The following are available online at www.mdpi.com/2072-666X/6/10/1436/s1, Figure S1: Detailed experimental setup. (a) Image of the experimental setup for observation of the capillary jet depicted in Figure 1; (b) Image of the acrylic holder in the CDS. The capillary was positioned in the holder, Table S1: Materials property, Table S2: Physical values at the transition from the dripping to the jetting regime.

Acknowledgments: We thank Yukiko T. Matsunaga for support in the experimental measurements. This work was partially supported by a Grant-in-Aid for Challenging Exploratory Research (Project No. 24651159) and a Grant-in-Aid for Scientific Research (S) (Project No. 22220001) from the Japan Society for the Promotion of Science (JSPS), Japan.

Author Contributions: K.M developed the concept of the paper. K.M and H.O designed the experimental setup. K.M collected and analyzed the experimental data. K.M wrote the manuscript with inputs from H.O, M.T and S.T. S.T supervised the overall coordination. All authors contributed to the manuscript and the interpretation of the data.

Conflicts of Interest: The authors declare no conflict of interest.

References

1. Pregibon, D.C.; Toner, M.; Doyle, P.S. Multifunctional encoded particles for high-throughput biomolecule analysis. *Science* **2007**, *315*, 1393–1396. [[CrossRef](#)] [[PubMed](#)]

2. Kim, D.H.; Rozhkova, E.A.; Ulasov, I.V.; Bader, S.D.; Rajh, T.; Lesniak, M.S.; Novosad, V. Biofunctionalized magnetic-vortex microdiscs for targeted cancer-cell destruction. *Nat. Mater.* **2010**, *9*, 165–171. [[CrossRef](#)] [[PubMed](#)]
3. Morimoto, Y.; Tan, W.H.; Tsuda, Y.; Takeuchi, S. Monodisperse semi-permeable microcapsules for continuous observation of cells. *Lab Chip* **2009**, *9*, 2217–2223. [[CrossRef](#)] [[PubMed](#)]
4. Kim, S.H.; Jeon, S.J.; Jeong, W.C.; Park, H.S.; Yang, S.M. Optofluidic synthesis of electroresponsive photonic janus balls with isotropic structural colors. *Adv. Mater.* **2008**, *20*, 4129–4134. [[CrossRef](#)]
5. Xu, Q.B.; Hashimoto, M.; Dang, T.T.; Hoare, T.; Kohane, D.S.; Whitesides, G.M.; Langer, R.; Anderson, D.G. Preparation of monodisperse biodegradable polymer microparticles using a microfluidic flow-focusing device for controlled drug delivery. *Small* **2009**, *5*, 1575–1581. [[CrossRef](#)] [[PubMed](#)]
6. Matsunaga, Y.T.; Morimoto, Y.; Takeuchi, S. Molding cell beads for rapid construction of macroscopic 3d tissue architecture. *Adv. Mater.* **2011**, *23*, H90–H94. [[CrossRef](#)] [[PubMed](#)]
7. Garstecki, P.; Fuerstman, M.J.; Stone, H.A.; Whitesides, G.M. Formation of droplets and bubbles in a microfluidic t-junction—Scaling and mechanism of break-up. *Lab Chip* **2006**, *6*, 437–446. [[CrossRef](#)] [[PubMed](#)]
8. Takeuchi, S.; Garstecki, P.; Weibel, D.B.; Whitesides, G.M. An axisymmetric flow-focusing microfluidic device. *Adv. Mater.* **2005**, *17*, 1067–1072. [[CrossRef](#)]
9. Maeda, K.; Onoe, H.; Takinoue, M.; Takeuchi, S. Controlled synthesis of 3D multi-compartmental particles with centrifuge-based microdroplet formation from a multi-barrelled capillary. *Adv. Mater.* **2012**, *24*, 1340–1346. [[CrossRef](#)] [[PubMed](#)]
10. Ambravaneswaran, B.; Subramani, H.J.; Phillips, S.D.; Basaran, O.A. Dripping-jetting transitions in a dripping faucet. *Phys. Rev. Lett.* **2004**, *93*, 034501. [[CrossRef](#)] [[PubMed](#)]
11. Clanet, C.; Lasheras, J.C. Transition from dripping to jetting. *J. Fluid Mech.* **1999**, *383*, 307–326. [[CrossRef](#)]
12. Rubio-Rubio, M.; Sevilla, A.; Gordillo, J.M. On the thinnest steady threads obtained by gravitational stretching of capillary jets. *J. Fluid Mech.* **2013**, *729*, 471–483. [[CrossRef](#)]
13. Tate, T. XXX. On the magnitude of a drop of liquid formed under different circumstances. *Philos. Mag. Ser. 4* **1864**, *27*, 176–180.
14. Rayleigh, L. On the capillary phenomena of jets. *Proc. R. Soc. Lond.* **1879**, *29*, 71–97. [[CrossRef](#)]
15. Utada, A.S.; Fernandez-Nieves, A.; Stone, H.A.; Weitz, D.A. Dripping to jetting transitions in coflowing liquid streams. *Phys. Rev. Lett.* **2007**, *99*, 094502. [[CrossRef](#)] [[PubMed](#)]
16. Ambravaneswaran, B.; Wilkes, E.D.; Basaran, O.A. Drop formation from a capillary tube: Comparison of one-dimensional and two-dimensional analyses and occurrence of satellite drops. *Phys. Fluids* **2002**, *14*, 2606–2621. [[CrossRef](#)]
17. Lister, J.R.; Stone, H.A. Capillary breakup of a viscous thread surrounded by another viscous fluid. *Phys. Fluids* **1998**, *10*, 2758–2764. [[CrossRef](#)]
18. Scheele, G.F.; Meister, B.J. Drop formation at low velocities in liquid-liquid systems. I. Prediction of drop volume. 2. Prediction of jetting velocity. *AIChE J.* **1968**, *14*, 9–15. [[CrossRef](#)]
19. Batchelor, G.K. *An Introduction in Fluid Dynamics*; Cambridge University Press: Cambridge, UK, 1967.
20. Tan, W.H.; Takeuchi, S. Monodisperse alginate hydrogel microbeads for cell encapsulation. *Adv. Mater.* **2007**, *19*, 2696–2701. [[CrossRef](#)]
21. Sahni, V.; Blackledge, T.A.; Dhinojwala, A. Changes in the adhesive properties of spider aggregate glue during the evolution of cobwebs. *Sci. Rep.* **2011**, *1*, 41. [[CrossRef](#)] [[PubMed](#)]
22. Meister, B.J.; Scheele, G.F. Drop formation from cylindrical jets in immiscible liquid systems. *AIChE J.* **1969**, *15*, 700–706. [[CrossRef](#)]
23. Eggers, J. Nonlinear dynamics and breakup of free-surface flows. *Rev. Modern Phys.* **1997**, *69*, 865–929. [[CrossRef](#)]
24. Ganan-Calvo, A.M.; DePonte, D.P.; Herrada, M.A.; Spence, J.C.H.; Weierstall, U.; Doak, R.B. Liquid capillary micro/nanojets in free-jet expansion. *Small* **2010**, *6*, 822–824. [[CrossRef](#)] [[PubMed](#)]
25. Sevilla, A. The effect of viscous relaxation on the spatiotemporal stability of capillary jets. *J. Fluid Mech.* **2011**, *684*, 204–226. [[CrossRef](#)]

